

# Robust Lyapunov-based Control of MEMS Optical Switches

Mohammad Goodarzi<sup>1\*</sup>

<sup>1</sup>Department of Electrical Engineering, Faculty of Engineering, Garmsar branch, Islamic Azad University, Garmsar, Iran

\*Email of Corresponding Author: m\_goodarzi181@yahoo.com

*Received: August 30, 2015; Accepted: December 27, 2015*

## Abstract

In this paper, a robust PID control scheme is proposed for Micro-Electro-Mechanical-Systems (MEMS) optical switches. The proposed approach is designed in a way which solves two challenging and important problems. The first one is successful reference tracking and the second is mitigating the system nonlinearities. The overall system composed of nonlinear MEMS dynamics and the PID controller is proven to be uniformly-ultimately bounded (UUB) stable in agreement with Lyapunov's direct method in any finite region of the state space. Since the unmodeled but bounded dynamics of the system is systematically encapsulated in the system model, the only influence that this imposes on the stability is the respective bounds on the controller gains. The controller design strategy is simple and practicable with low computation burden which makes it easy to apply for control of MEMS optical switch. It also forms a constructive and conservative algorithm for suitable choice of gains in PID controller. The effectiveness of the proposed control law is verified through simulations in MATLAB/SIMULINK. It is shown that the proposed control law ensures robust stability and performance despite the modeling uncertainties.

## Keywords

Robust PID control, Uniformly-ultimately bounded (UUB) stability, Micro-Electro Mechanical Systems (MEMS), Lyapunov stability

## 1. Introduction

Micro-Electro-Mechanical-Systems are emerging systems with ever-increasing applications in modern industries. MEMS technology can be utilized to produce complex structures, devices and systems in the micrometer scale [1, 2]. They have enabled many types of sensors, actuators and systems to be reduced in size by several orders of magnitude, while at the same time improve their performances [3]. One of the fields that undergo rapid miniaturization is that of optical signal transmission [4]. Bandwidth is limited by large-scale matrix switches, requiring signal conversion from optical, to electronic, and reverse. One solution to this problem is utilizing MEMS optical switches to perform switching operations. MEMS optical switches manipulate optical signals directly, without having to first converting them to electronic signals with lower size and power consumption [5]. This is important whereas telecommunication industry's desire to focus on all-optical networks, meaning total exclusion of signal conversion in optical signal transmission. The considerable point is that, although, the advances in micromachining technology make it possible for large-scale matrix switches to be monolithically integrated on a single chip [6], there are yet several problems.

-MEMS models suffer from nonlinearities and uncertainties like many other dynamical systems.

-Unlike macro mechanical systems where the dynamic modeling is relatively simple, it is quite problematic in the MEMS case. Damping rate is the parameter, which is difficult to determine analytically, even through finite element analysis [7]. The presence of high-frequency system dynamics is also introduced as additional challenge for the MEMS dynamic modeling that increases the systems' complexity and so invokes appropriate controllers to cope with this issue.

A lot of researchers have focused on some possible solutions to overcome the aforementioned weaknesses [4, 8-15]. [12] proposed a robust fault detection and fault-tolerant-control (FTC) system for an uncertain nonlinear MEMS optical switch. Considering the earlier works, it shows that, almost, all the presented approaches require fair prior knowledge about the complex dynamics of MEMS for the controller design procedure. This weakness can be partly eliminated by using Fuzzy/neural Network (NN) based control approaches [16]. Neural Networks provide powerful abilities such as adaptive learning, parallelism, fault tolerance, and generalization to the fuzzy controller. However, it is very difficult to guarantee the stability and robustness of Neural Network control systems [17-19]. These problems together computational limitations supersede the desire to apply advanced controllers in the micro scale objects. It is because the control scheme should have a cheap and simple structure, due to realization in CMOS technology.

To tackle these problems, several other works have been proposed. In [20], a robust controller for the MEMS optical switch using Quantitative feedback theory is proposed. In [21], a comparison of three robust control strategies (sliding-mode, high-gain and model-free control) is presented. The proposed model-free approach uses only a simple linear model of the system so-called "available model" and all the rest of dynamics are treated as external disturbances. It also considers the actual external disturbances in addition to the uncertainties caused by the parameter uncertainties.

This paper presents a robust PID controller for the MEMS optical switch. It is found that with minimum implementation complexity, the proposed approach speeds up the system response, improves its dynamical behavior, and renders much less sensitivity to the parameter changes. It also ensures robust stability and excellent performance in presence of nonlinear and unknown modeling uncertainties. This paper is organized as follows. In section 2, dynamic modeling and some preliminaries are described. The plant parameters are assumed to be uncertain, but with known upper and lower bounds, in this section. The control scheme derivation and stability analysis are presented in Section 3. Section 4 is devoted to the numerical evaluation of the controller on a MEMS optical switch. Finally, section 5 offers a brief summary and conclusions.

## **2. MEMS Switches Dynamical Model**

The scanning electron microscope (SEM) micrograph of the MEMS optical switch composed of an electrostatic comb drive actuator, a suspension beam, and reflection micromirror with optical fiber grooves is shown in Figure 1.

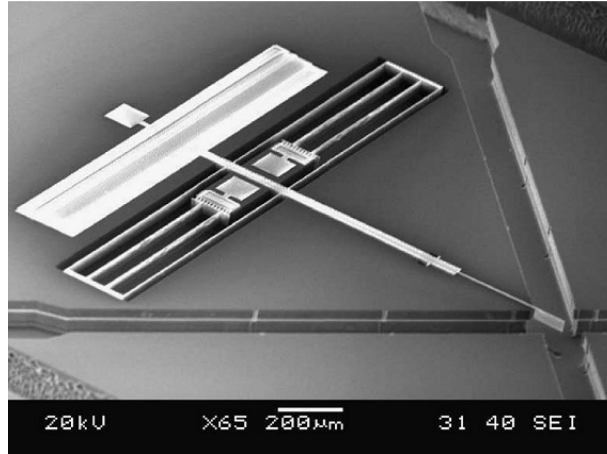


Figure1. SEM image of a MEMS optical switch [5]

Optical fibers will be inserted into the fiber grooves and deliver the light from one input to another output. Without external voltage, the mirror is in the beam path and the incident signal from input fiber is reflected by the mirror into the output fiber, the switch is at the cross state. When the actuator is applied by a proper driving voltage, the electrostatic force induced by the actuator will drive the shuttle and so the attached micro mirror out of the beam path. As a consequence, the incident beam will be transmitted directly into the other output fiber, where the switch is at bar state. When the voltage is released, the mirror will latch to the original position and the cross state is recovered [5]. In order to obtain the dynamic equations of MEMS optical switch, one needs to determine all forces, electrostatic and mechanical, acting on the shuttle. It is assumed that, the shuttle has one degree of freedom and other situations, for instance, rotation around the main body axes, translational along them, as well as different vibration modes that impose additional degrees of freedom are not considered here. Finally, the optical model will be achieved. We will perform this derivation in three steps.

*Step1:* In order to obtain the model of electrostatic force between the two comb drive electrodes, first the capacitance of the comb drive should be determined as a function of position. The capacitance is calculated as a sum of parallel capacitances among pairs of comb electrodes. The total capacitance, as a function of the position  $x$ , is given as [5,14].

$$C(x) = \frac{2n\epsilon_0 T(x+x_0)}{d} \tag{1}$$

Where  $n$  is the number of the movable comb fingers,  $\epsilon_0 = 8.85 \times 10^{-12} F/m$  is the permittivity or dielectric constant for free space,  $T$  and  $d$  are the thickness of the finger and the gap between fingers, respectively,  $x$  is the shuttle position, and  $x_0$  is the initial overlapping between the electrodes. The electrostatic force between the electrodes of the capacitor is then given by [7, 14].

$$f(v, x) = \frac{1}{2} v^2 \frac{\partial C}{\partial x} \tag{2}$$

Substitute the total capacitance denoted by (1) into (2) to get the following relation for the electrostatic force:

$$f(v, x) = \frac{n\epsilon_0 T}{d} v^2 = k_e v^2 \tag{3}$$

Where  $k_e$  is the input gain and  $v$  denotes the voltage applied over terminals of the comb drive electrodes.

Remark 1: The electrostatic force depends only on the voltage across the capacitor not on the position. It returns to the linearity between the capacitance and the position over a wide range of deflections that is the most important characteristics of the comb drive.

Step2: Here, we will obtain mechanical forces imposed to the shuttle. It consists of two elements. The first one is the so-called stiffness of the suspension mechanism, and the second one is a function describing losses such as damping and friction.

The stiffness of the suspension is assumed to be a linear function of the position and its coefficient is given by [5].

$$k_x = 2ET \left(\frac{BW}{BL}\right)^3 \tag{4}$$

Where  $E$  is Young's modulus,  $BW$  is the width of suspension beams,  $BL$  is its length, and  $T$  is its thickness.

As mentioned before, damping is the most difficult parameter to determine analytically, even through finite element analysis (FEA). The reason lies in the number of different mechanisms that causes it, including friction, viscous forces, drag, etc [7]. Generally, they can be defined as [4].

$$d(x, \dot{x}) = \frac{\eta}{2\epsilon_0} C(x) \dot{x} = (d_x \dot{x} + d_0) \dot{x} \tag{5}$$

Where  $\eta$  is velocity of the air surrounding switch.

Now, according to the last steps, and utilizing the Newton's second law, the motion equation of the MEMS optical switch is obtained as:

$$m\ddot{x} = k_e v^2 - d(x, \dot{x}) - k_x x \tag{6}$$

Where  $m = m_{mirror} + 0.5m_{rigid} + 2.74m_{beam}$  is the effective moving mass of the shuttle. For simplicity in notation, the system representation (6) can also be written in a compact form as follows:

$$m\ddot{x} + N(x, \dot{x}) = k_e u \tag{7}$$

In which  $N(x, \dot{x}) = d(x, \dot{x}) + k(x)$ , and  $u = v^2$  indicates the variable for which we intend to design a control according to the voltage.

Step3: Here, we will achieve the optical model for MEMS optical switch. It is simply a function that connects the intensity of light to the position of the blade, as shown in Figure 2.

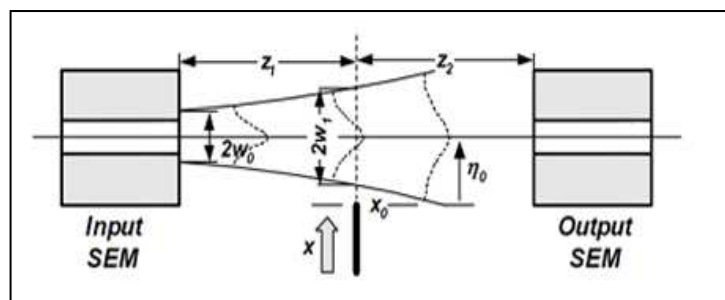


Figure2. Optical model [5]

The light beam is intercepted by the blade, increasing and decreasing the through put of light. The Rayleigh-Sommerfeld model is based on a Gaussian distribution of the intensity across the light beam. The waist of the Gaussian beam coming from the fiber is  $w_0$ . As the beam propagates in free space the waist  $w_1$  is given as

$$w_1 = w_0 \sqrt{1 + \left(\frac{z_1}{z_R}\right)^2}, \quad z_R = \frac{\pi w_0^2}{\lambda} \quad (8)$$

With  $w_0 = 5.1\mu m$ ,  $z_1 = 10\mu m$ , and  $\lambda = 1.55\mu m$ . The transmitted power can then be described as

$$P = h(x) = 0.5 \left( 1 - \operatorname{erf} \left( \frac{\sqrt{2}(x - \eta_0)}{w_1} \right) \right) \quad (9)$$

Where  $\eta_0$  denotes the distance from the fiber axis. For a good survey, the reader may study [14]. In summary, the complete dynamic equations of the MEMS optical switch can be described by (5) and (9). The terms of such a dynamical model satisfy some properties. Some of them are recalled here.

*Property1:* The effective mass for the switch  $m$  satisfies  $0 < \underline{m} \leq m \leq \bar{m}$ , where  $\underline{m}$  and  $\bar{m}$  are positive scalars representing the lower and upper bounds, respectively.

*Property2:* The damping function  $d(x, \dot{x})$  satisfies  $|d(x, \dot{x})| \leq (\bar{d}_0 + \bar{d}_x |x|) |\dot{x}|$ ,  $\forall x, \dot{x} \in \square$ , for some positive constants  $\bar{d}_0$  and  $\bar{d}_x$ .

*Property3:* The Stiffness vector satisfies  $|k(x)| \leq \bar{k}_x |x|$ ,  $\forall x \in \square$ , for some positive constant  $\bar{k}_x$ .

### 3. Robust PID control of MEMS optical switch

In this section, considering uncertainties in the MEMS model, a robust PID controller is proposed based on the bounds of dynamical terms of the motion equations and then its robust stability is analyzed with respect to the model uncertainties. In the stability analysis, it is assumed that the dynamical terms  $m$ ,  $d(x, \dot{x})$  and other terms are uncertain and there is only some information about their bounds. With this in mind, recall the dynamic model of system (5). The PID control law is given by

$$u = k_d \dot{e} + k_p e + k_I \int_0^t e(\sigma) d\sigma \quad (10)$$

where  $e = x_d - x$  denotes the position error,  $x_d$  stands for the desired position of optical switch and  $k_p$ ,  $k_d$  and  $k_I$ , are real positive scalars chosen by the designer to satisfy certain conditions. Substitute the control law denoted by (10) into (5) to get the following relation for the closed- loop system:

$$\dot{y} = \mathbf{A}y + \mathbf{B}\Delta \mathbf{A} \quad (11)$$

in which

$$\mathbf{A} = \begin{bmatrix} 0 & 1 & 0 \\ 0 & 0 & 1 \\ -m^{-1}k_e k_I & -m^{-1}k_e k_p & -m^{-1}k_e k_d \end{bmatrix},$$

$$\mathbf{B} = \begin{bmatrix} 0 \\ 0 \\ m^{-1} \end{bmatrix}, \quad y = \begin{bmatrix} \int_0^t e(\sigma) d\sigma & e & \dot{e} \end{bmatrix}^T \quad (12)$$

$$\Delta \mathbf{A} = m\ddot{x}_d + N(x, \dot{x})$$

Before stating the stability results, we present the following lemma.

*Lemma 1.* Assume that the following properties hold for Lyapunov function of a dynamic system:

$$\underline{v} \|\mathbf{x}\|^2 \leq V(\mathbf{x}) \leq \bar{v} \|\mathbf{x}\|^2 \quad (13)$$

$$\dot{V}(\mathbf{x}) \leq \|\mathbf{x}\|(\sigma_0 - \sigma_1 \|\mathbf{x}\| + \sigma_2 \|\mathbf{x}\|^2)$$

Where  $\underline{v}$ ,  $\bar{v}$  are the largest and smallest Eigen values of  $V(\mathbf{x})$ , respectively, and  $\sigma_i$  ( $i=0,1,2$ ) are constants. Given that

$$d = \frac{2\sigma_0}{\sigma_1 + \sqrt{\sigma_1^2 - 4\sigma_0\sigma_2}} \sqrt{\frac{\bar{v}}{\underline{v}}} \quad (14)$$

Then the system with the initial condition  $\mathbf{x}_0$  is UUB with respect to  $B(0, d)$ , provided that

$$\sigma_1 > 2\sqrt{\sigma_0\sigma_2} \quad (15)$$

$$\sigma_1^2 + \sigma_1 \sqrt{\sigma_1^2 - 4\sigma_0\sigma_2} > 2\sigma_0\sigma_2 \left(1 + \sqrt{\frac{\bar{v}}{\underline{v}}}\right) \quad (16)$$

$$\sigma_1 + \sqrt{\sigma_1^2 - 4\sigma_0\sigma_2} > 2\sigma_2 \|\mathbf{x}_0\| \sqrt{\frac{\bar{v}}{\underline{v}}} \quad (17)$$

where  $\|\mathbf{x}_0\|$  represents an upper bound on the initial condition  $\mathbf{x}_0$ .

Proof: Proof can be found in [22] under 3.1.

### 3.1 Stability analysis

To analyze the robust stability of the system, consider the following Lyapunov function candidate

$$V(y) = y^T \mathbf{P}y \quad (18)$$

in which

$$\mathbf{P} = \frac{1}{2} \begin{bmatrix} \alpha_2 k_p + \alpha_1 k_I + \alpha_2^2 m & \alpha_2 k_d + k_I + \alpha_1 \alpha_2 m & \alpha_2 m k_e^{-1} \\ \alpha_2 k_d + k_I + \alpha_1 \alpha_2 m & \alpha_1 k_d + k_p + \alpha_1^2 m & \alpha_1 m k_e^{-1} \\ \alpha_2 m & \alpha_1 m & m k_e^{-1} \end{bmatrix} \quad (19)$$

where  $\alpha_1$  and  $\alpha_2$  are positive scalars and  $\alpha_1 + \alpha_2 < k_e^{-1}$ . Now we can conclude on the positive definiteness of matrix  $\mathbf{P}$  as follows.

*Lemma 2.* Assume the following inequalities hold:

$$\alpha_1, \alpha_2 > 0 \quad , \quad \alpha_1 + \alpha_2 < k_e^{-1} \quad (20)$$

$$s_1 = \alpha_2(k_p - k_d) - (1 - \alpha_1)k_I - \alpha_2(k_e^{-1} + \alpha_1 - \alpha_2)\bar{m} > 0 \quad (21)$$

$$s_2 = k_p + (\alpha_1 - \alpha_2)k_d - k_I - \alpha_1(k_e^{-1} + \alpha_2 - \alpha_1)\bar{m} > 0 \quad (22)$$

Then,  $\mathbf{P}$  is positive definite and satisfies:

$$\underline{\lambda}(\mathbf{P})\|y\|^2 \leq V(y) \leq \bar{\lambda}(\mathbf{P})\|y\|^2 \quad (23)$$

in which

$$\bar{\lambda}(\mathbf{P}) = \max\left\{\left(\frac{k_e^{-1} + \alpha_1 + \alpha_2}{2}\bar{m}\right), \frac{s_3}{2}, \frac{s_4}{2}\right\} \quad (24)$$

$$\underline{\lambda}(\mathbf{P}) = \min\left\{\left(\frac{k_e^{-1} - \alpha_1 - \alpha_2}{2}m\right), \frac{s_1}{2}, \frac{s_2}{2}\right\}$$

with

$$s_3 = \alpha_2(k_p + k_d) + (1 + \alpha_1)k_I + (k_e^{-1} + \alpha_1 + \alpha_2)\bar{m}\alpha_2 \quad (25)$$

$$s_4 = \bar{m}\alpha_1(k_e^{-1} + \alpha_2 + \alpha_1) + k_d(\alpha_1 + \alpha_2) + k_p + k_I \quad (26)$$

$\bar{m}$  and  $m$  are defined before in property 1.

Proof: proof is based on Gershgorin theorem [23].

Now, when  $\mathbf{P}$  is positive definite then we can conclude on the negative definiteness of the Lyapunov function (15). By differentiating (15) with respect to time we have

$$\begin{aligned} \dot{V}(y) = & -y^T H y + \frac{1}{2} y^T \begin{bmatrix} 0 & m\alpha_2^2 & m\alpha_1\alpha_2 \\ m\alpha_2^2 & 2m\alpha_1\alpha_2 & m\alpha_1^2 + m\alpha_2 k_e^{-1} \\ m\alpha_1\alpha_2 & m\alpha_1^2 + m\alpha_2 k_e^{-1} & 2m\alpha_1 k_e^{-1} \end{bmatrix} y \\ & + y^T \begin{bmatrix} \alpha_2 k_e^{-1} \\ \alpha_1 k_e^{-1} \\ k_e^{-1} \end{bmatrix} \Delta \mathbf{A} \end{aligned} \quad (27)$$

Where

$$H = \begin{bmatrix} \alpha_2 k_I & 0 & 0 \\ 0 & \alpha_1 k_p - \alpha_2 k_d - k_I & 0 \\ 0 & 0 & k_d \end{bmatrix} \quad (28)$$

Thus

$$\dot{V}(y) \leq -\gamma \|y\|^2 + \bar{m} \lambda_1 \|y\|^2 + \|y\| \left\| \begin{bmatrix} \alpha_2 k_e^{-1} \\ \alpha_1 k_e^{-1} \\ k_e^{-1} \end{bmatrix} \right\| \|\Delta \mathbf{A}\| \quad (29)$$

With

$$\gamma = \min\{\alpha_2 k_I, \alpha_1 k_p - \alpha_2 k_d - k_I, k_d\} \quad (30)$$

Now, from properties 1-3 we have

$$\|\Delta \mathbf{A}\| \leq \beta_0 + \beta_1 \|y\| + \beta_2 \|y\|^2 \quad (31)$$

This in turn gives

$$\dot{V}(y) \leq \|y\| (\phi_0 - \phi_1 \|y\| + \phi_2 \|y\|^2) \quad (32)$$

In which

$$\phi_0 = \beta_0 \lambda_2, \quad \phi_1 = \gamma - \bar{m} \lambda_{\max}(\mathbf{R}) - \beta_1 \lambda_2, \quad \phi_2 = \beta_2 \lambda_2 \quad (33)$$

And  $\lambda_{\max}$  denotes the maximum eigen value of the matrix. Furthermore

$$\lambda_2 = \left\| \begin{bmatrix} \alpha_2 \\ \alpha_1 \\ 1 \end{bmatrix} \right\| \times k_e^{-1}, \quad \mathbf{R} = \frac{1}{2} \begin{bmatrix} 0 & \alpha_2^2 & \alpha_1 \alpha_2 \\ \alpha_2^2 & 2\alpha_1 \alpha_2 & \alpha_1^2 + \alpha_2 k_e^{-1} \\ \alpha_1 \alpha_2 & \alpha_1^2 + \alpha_2 k_e^{-1} & 2\alpha_1 k_e^{-1} \end{bmatrix} \quad (34)$$

Now, we present the following theorem.



Theorem 1. The error system (8) is stable of the form of Uniformly Ultimately Bounded (UUB), if  $\phi_1$  is chosen large enough.

Proof. According to Eq (20) and Lemma 1, if the following conditions hold, the system is UUB stable. The conditions are

$$\phi_1 > 2\sqrt{\phi_0\phi_2} \tag{35}$$

$$\phi_1^2 + \phi_1\sqrt{\phi_1^2 - 4\phi_0\phi_2} > 2\phi_0\phi_2\left(1 + \sqrt{\frac{\bar{\lambda}(\mathbf{P})}{\underline{\lambda}(\mathbf{P})}}\right) \tag{36}$$

$$\phi_1 + \sqrt{\phi_1^2 - 4\phi_0\phi_2} > 2\phi_2\|y_0\|\sqrt{\frac{\bar{\lambda}(\mathbf{P})}{\underline{\lambda}(\mathbf{P})}} \tag{37}$$

These conditions can be simply met by enlarging  $\phi_1$  through picking suitable feedback gains  $k_p, k_I,$  and  $k_d,$  and this completes the proof.

Remark 2: The uniform ultimate boundedness result is of local nature, because the condition (33) depends on the initial condition  $y_0$ . Nonetheless, it is important to observe that these conditions can be met for an arbitrary  $y_0$ . In modern terminology, this kind of stability is called semi-global.

The following steps can be used as guidelines for the actual implementation of the control system (8).

- Determinate the MEMS-specific quantities  $\bar{m}, \underline{m}, \bar{d}_0, \bar{d}_x$  and  $\bar{k}_x$ .
- Specify upper bounds on the desired position, velocity and acceleration.
- Find the corresponding  $\beta_0, \beta_1$  and  $\beta_2$  by the last two steps.
- Taking (20) into consideration, select  $\alpha_1$  and  $\alpha_2$ , and compute  $\lambda_2$ .
- Obtain  $\phi_0$ , and  $\phi_2$  from (31).
- Choose  $\phi_1$  according to (33).
- Fix an upper bound on the initial error state  $y_0$ .
- Calculate  $\gamma$  from (31), and choose  $k_p, k_I,$  and  $k_d$  to satisfy the requirement of robust stability.

Next, the usefulness of the presented approach is shown by some numerical examples.

#### 4. Simulation results

For illustrative purposes, a second order MEMS optical switch is considered, whose parameters are given in Table 1.

Table1. The MEMS parameters

$k_x = 0.6 \pm 0.12 \text{ Nm}^{-1}$	$d_x = 0.0363 \pm 0.00726$	$d_0 = (4.5 \pm 0.9) \times 10^{-3} \text{ Ns}$
$k_e = (1.9 \pm 0.38) \times 10^{-8} \text{ N/V}^2$	$m = 2.35 \times 10^{-9} \text{ kg}$	$d = 2.6 \mu\text{m}$

This model is based on empirical measurements and serves to provide a plant that mimics real world components. The simulation model is supposed to be driven by a uni-polar voltage source, whose amplitude is limited by a saturation block to 0 and 35 volt. The goal of the controller is to move shuttle from an initial position to a new desired one and reverse. The control parameters were set to be  $\alpha_1 = 1.85$  and  $\alpha_2 = 1.25$ ,  $k_p = 4 \times 10^{10}$ ,  $k_I = 2 \times 10^9$ , and  $k_d = 2 \times 10^8$ . According to these, the long displacement of the actuator has been shown in Figure 3. As can be seen, the proposed controller responds to the desired trajectory well.

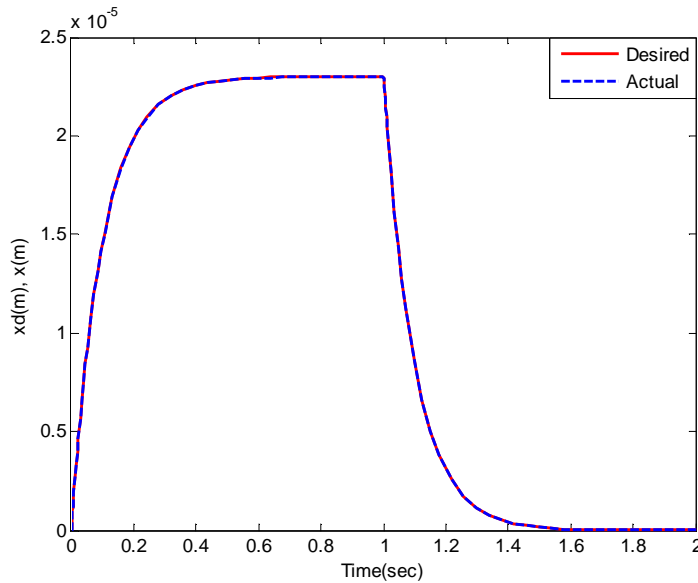


Figure3. Responses of the system to desired filtered trajectory

The control effort is also limited as shown in Figure 4.

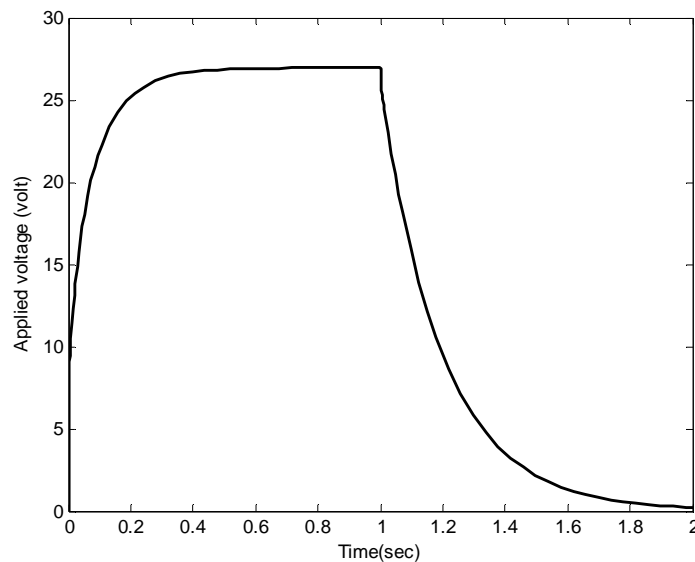


Figure4. Input voltages

The next simulations were carried out to investigate the control performance when the reference input is given by  $x_d = 11.75 \times (1 - \cos(0.5\pi t)) \mu m$ . The control parameters were selected as previous to satisfy the stability conditions. Figure5 and Figure 6 give the system responses, and the applied voltage, respectively.

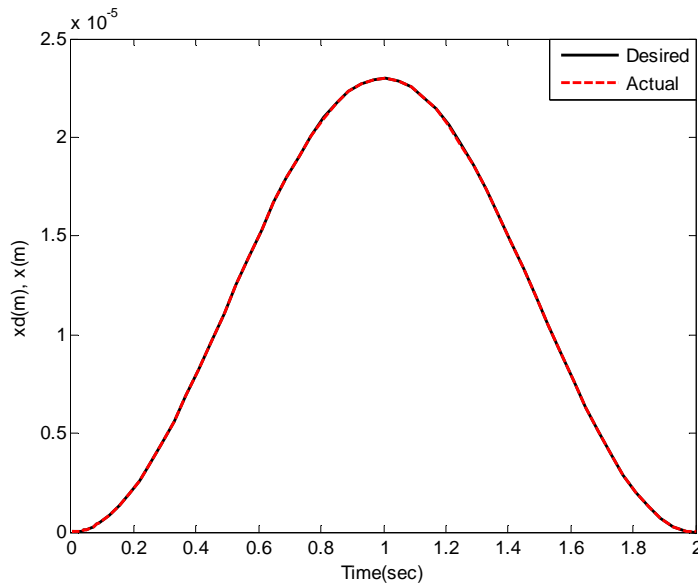


Figure5. The system responses

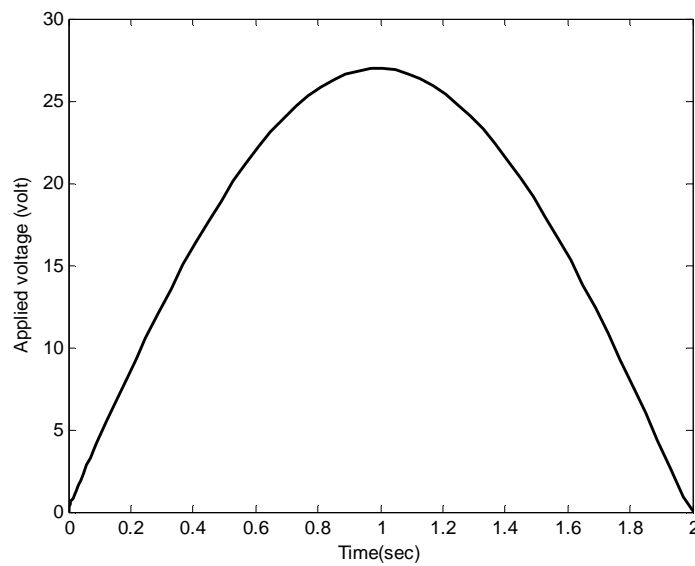


Figure6. Input voltage

As can be seen, the proposed controller responds to the desired trajectory promptly and steadily. Hence, it is straightforward to draw the conclusion that the system under control is potentially stable by choosing suitable gains satisfying the conditions (33) to (34) even in the presence of system uncertainties.

## 5. Conclusion

A Robust PID controller is proposed to overcome uncertainties of MEMS optical switches. The control laws have been derived under the assumption that some information about uncertainties' upper/lower bounds are in hand. The system stability has been verified by the Lyapunov method. The controller design strategy is simple and practicable with low computation burden which makes it easy to apply for control of MEMS optical switch. Simulation results have demonstrated that the control system is robust with the presence of uncertainties including modeling errors and external disturbances.

## 6. References

- [1] Parsi, B., Bahrami, M., Monemian Esfahani, A. and SeyedzadehSany, B. 2013. Calibration verification of a low-cost method for MEMS accelerometers. Transactions of the Institute of Measurement and Control. 0142331213513607.
- [2] Lu, M. S. C. and Fedder, G. 2004. Position control of parallel-plate micro actuators for probe-based data storage. Journal of Microelectromech. System, 13(5), 759-769.
- [3] Vagia, M. and Tzes, A. 2007. Robust PID control design for an electrostatic micromechanical actuator with structural uncertainty. IET control Theory and Applications. 2(5), 365-373.
- [4] Borovic, B., Hong, C., Liu, A. Q., Xie, L. and Lewis, F. L. 2004. Control of a MEMS optical switch. 43rd IEEE Conf. on Decision and Control, 3039-3044.
- [5] Li, J., Zhang, Q. X. and Liu, A. Q. 2003. Advanced fiber optical switches using deep RIE (DRIE) fabrication. Sensors and Actuators A., 102(3), 286-295.
- [6] Chen, R. T., Nguyen, H. and Wu, M. C. 1999. A high-speed low-voltage stress-induced micromachined 2x2 optical switch. IEEE Photonics Technology Letters., 11(11).
- [7] Khayatzaheh Safaie, B., Shamshirsaz, M. and Bahrami, M. 2014. Robust design under uncertainties of electro-thermal microactuator. Symposium on Design, Test, Integration & Packaging of MEMS/MOEMS, 1-6.
- [8] Park, J., Wang, L., Dawson, J. M., Hornak, L. A. and Famouri, P. 2005. Sliding mode-based microstructure torque and force estimations using MEMS optical monitoring. IEEE Sensors Journal., 5(3), 546-552.
- [9] Zhu, G., L'evine, J. and Praly, L. 2005. On the differential flatness and control of electrostatically actuated MEMS. American Control Conference, 2493-2498.
- [10] Huang, X., Horowitz, R. and Li, Y. 2005. Design and analysis of robust track-following controllers for dual-stage servo systems with an instrumented suspension. American Control Conference, 1126-1131.
- [11] Zhu, G., Penet, J. and Saydy, L. 2006. Robust control of an electrostatically actuated MEMS in the presence of parasitics and parametric uncertainties. Proceedings of the American Control Conference, 1233-1238.
- [12] Saif, M., Ebrahimi, B. and Vali, M. 2012. A second order sliding mode strategy for fault detection and fault-tolerant-control of a MEMS optical switch. Mechatronics., 22(6), 696-705.
- [13] Fei, J. and Batur, C. 2007. A novel adaptive sliding mode controller for MEMS gyroscope. 46th IEEE Conference on Decision and Control, USA, 3573-3578.

- [14] Borovic, B., Liu, A. Q., Popa, D., Cai, H. and Lewis, F. L. 2005. Open-loop versus closed-loop control of MEMS devices: choices and issues. *J. Micromechanics, Microengineering.*, 15(10), 1917-1924.
- [15] Jagannathan, S. and Yang, Q. 2005. A Robust controller for the manipulation of micro-scale objects. *American Control Conference*, 4154-4159.
- [16] Bahrami , M. Imani, A., Ghanbari, A. and Ebrahimi, B. Robust control of a MEMS optical switch using fuzzy sliding mode. 2011. 2nd International Conference on Control, Instrumentation and Automation (ICCIA), 396-400
- [17] Izadbakhsh, A., Akbarzadeh Kalat, A., Fateh, M. M. and Rafiei, S.M.R. 2011. A robust Anti-Windup control design for electrically driven robots-Theory and Experiment. *International Journal of Control. Automation, and Systems*, 9(5), 1005-1012.
- [18] Izadbakhsh, A. and Fateh, M. M. 2014. Real-time Robust Adaptive control of Robots Subjected to Actuator Voltage Constraint. *Nonlinear Dynamics*, 78(3), 1999-2014.
- [19] Izadbakhsh, A. and Rafiei, S.M.R. 2009. Endpoint Perfect Tracking Control of Robots - A Robust Non Inversion-Based Approach. *International Journal of Control, Automation, and Systems*, 7(6), 888-898.
- [20] Torabi, K., Vali, M., Ebrahimi, B. and Bahrami, M. 2010. Robust control of Nonlinear MEMS optical switch based on quantitative feedback Theory. 5th IEEE International Conference on Nano/Micro Engineered and Molecular systems, 122-128.
- [21] Izadbakhsh, A. and Rafiei, S.M.R. 2008. Robust control methodologies for optical micro Electro mechanical system - New approaches and comparison. *Power Electronics and Motion Control Conf. 13th Power Electronics and Motion Control Conf. EPE-PEMC: 2102–2107.*
- [22] Qu, Z. and Dawson, D. 1996. *Robust Tracking Control of Robot Manipulators*. 1nd Edition, IEEE Press.
- [23] Stewart, G. W. 1973. *Introduction to matrix computations*. Academic press, New York.